

From Theory to Practice in Rail Geotechnology

B. Indraratna, S. Nimbalkar, N. Tennakoon & Q. D. Sun

Centre for Geomechanics and Railway Engineering; Program Leader, ARC Centre of Excellence for Geotechnical Science and Engineering; University of Wollongong, Wollongong City, NSW 2522, Australia

ABSTRACT: In recent times the increase in axle loads and train speeds have posed serious geotechnical issues with ballasted railway tracks, both in Australia and the world. The large deformations and degradation of ballast under cyclic and impact loads, and the low bearing capacity of compacted ballast and impaired drainage often exacerbate track maintenance. In recent times in Australia, geosynthetics have been trialed in ballasted tracks constructed on soft and saturated formations to help improve stability and longevity. Comprehensive field studies on instrumented tracks at Bulli (near Wollongong) and Singleton (near Newcastle) supported by RailCorp and ARTC, were carried out to measure the in-situ stresses and deformation of ballast embankments. The findings of the Bulli Study indicated that recycled ballast could be effectively reused in track construction if it was re-graded and reinforced with geocomposites. The results of the Singleton Study showed that geogrids with an optimum aperture size can significantly reduce deformations of ballast layer by providing improved interlock with the particles. It was also found that the strains accumulated in geogrids were influenced by deformation of the subgrade, whereas the induced transient strains were mainly affected by the stiffness of the geogrids. A better understanding of such performance would allow for a safer and more effective design and analysis of ballasted rail tracks with geosynthetic reinforcement and resilient shock mats.

KEY WORDS: Bearing capacity, ballast, fouling, geosynthetics, particle breakage.

1 INTRODUCTION

Ballasted rail tracks are popular because of their relatively low cost of construction and flexible maintenance. Ballast consists of gravel sized aggregates (10–60 mm) that ensures that the cyclic loads are safely transmitted to the capping (or formation soils), and that the track is anchored transversely and longitudinally. But when the ballast is not properly conditioned, it is also one of the main sources of deteriorating track geometry (Selig and Waters 1994). Under large repetitive (cyclic) train loads, ballast undergoes particle breakage and excessive deformation and subsequent track settlement, which means the ballast urgently needs multi-cycle track restoration in the form of cleaning or renewal. The characteristics required for ballast to achieve its main functions are clearly contradictory in some aspects, which means that a particular type of ballast cannot accomplish all of them completely (Profillidis, 1995). It could be argued that for high load-bearing characteristics and maximum track stability the ballast needs to be angular, well graded and compact, which in turn reduces the drainage of the track. Therefore a balance needs to be achieved between bearing capacity and drainage (Indraratna et al. 2006).

Geosynthetics can be used in new rail tracks and in track rehabilitation schemes to curtail future deformation. A number of laboratory tests on modelled tracks have been carried out and reductions of up to 30% in the vertical strains on the ballast layer stemming from geogrids and geocomposites have been reported (Bathurst and Raymond 1987, Raymond 2002, Brown et al. 2007, Indraratna et al. 2011b, Indraratna and Nimbalkar 2012). Geogrids can reduce the lateral spreading and fouling of ballast, as well as its degradation, especially in wet conditions. Aspiz et al. (2002) reported benefits from geotextile installed in the ballast layer in terms of it inhibiting lateral spreading. Moreover, non-woven geotextile also prevents fines moving up from the layers of sub-ballast and subgrade (subgrade pumping), which helps to keep the recycled ballast relatively clean, while shock mats mitigate the impact induced ballast degradation. Furthermore, the sub-ballast itself can act as a filter layer that minimises the adverse effects of clay pumping and hydraulic erosion originating from the subgrade. This keynote paper addresses a number of research areas, including the theoretical, laboratory, and field investigations, conducted at the Centre for Geomechanics and Railway Engineering (GRE) of the University of Wollongong, under the auspices of the CRC for Rail Innovation, and in collaboration with railway industries in Australia.

2 TRACK DRAINAGE AND FOULING

The primary purpose of track drainage is the rapid removal of water from the substructure in order to keep the load bearing stratum relatively dry. Water can penetrate into the load bearing stratum from four different sources (Indraratna et al. 2011b): (a) Precipitation (rain and snow), (b) Surface flow from adjacent hill slopes, (c) Upward seepage from the subgrade, and (d) A high groundwater table in low lying coastal regions.

Track substructure should be designed and constructed so as to drain the water into nearby drainage ditches or pipes, but as the track ages, fouling of ballast due to intrusion of fine material either from surface or subgrade slowly decreases its drainage capacity. In saturated tracks, poor drainage can lead to a build-up of excess pore water pressure under train loading. If the permeability of the layers of substructure becomes markedly low, train loading induces a considerable build up excess pore water pressure which is often not dissipated sufficiently before the next train load is applied. Thus, the residual pore pressure accumulates with increasing load cycles, which often leads to a drastic reduction in the load bearing capacity of the track.

Figure 1 shows rail tracks suffering from inadequate drainage. In the case of poor drainage, problems may occur in the track such as (i) reduced ballast shear strength, stiffness, and load bearing capacity, (ii) increased track settlement, (iii) softening of subgrade, (iv) formation of slurry and clay pumping under cyclic loading, (v) ballast attrition by jetting action and freezing of water, and (vi) sleeper degradation by water jetting. All these problems will degrade the performance of the track and demand additional maintenance.

In order to accurately measure the quantity of fouling, an index called Void Contaminant Index (VCI) can be used and is expressed as (Tennakoon et al. 2012, Indraratna et al. 2012):

$$VCI = \frac{(1 + e_f)}{e_b} \times \frac{G_{sb}}{G_{sf}} \times \frac{M_f}{M_b} \times 100 \quad (1)$$

where, e_b = void ratio of clean ballast, e_f = void ratio of fouling material, G_{sb} = specific gravity of clean ballast, G_{sf} = specific gravity of fouling material, M_b = dry mass of clean ballast, M_f = dry mass of fouling material. For example, a value of VCI = 50% indicates that half of the total voids in the ballast are occupied by the fouling material. More details of VCI including

field determination procedures are available in Tennakoon et al. (2012) and Indraratna et al. (2012).



Figure 1: Tracks suffering from poor drainage (Adopted from Lackenby, 2006)

2.1 Large Scale Permeability Tests

A series of large scale constant head permeability tests were conducted at the University of Wollongong to study the effect of fouling on hydraulic conductivity. This equipment (Figure 2) could accommodate ballast specimens 500 mm in diameter and 300-500 mm high. In this study clay fouling was simulated using kaolin as the fouling material. The initial density of fresh ballast was 15.98 kN/m^3 . Kaolin clay was mixed with fresh ballast and then placed in several layers which were subjected to compaction to maintain the density of the specimen.



Figure 2: Large scale permeability apparatus



Figure 3: Large scale triaxial apparatus

The results of the hydraulic conductivity values for different levels of clay fouling are presented in Table 1.

Table 1: Measured values of Hydraulic conductivity of clay-fouled ballast

Void Contaminant Index, VCI (%)	Hydraulic conductivity, k (m/s)
0	0.3
25	0.02
50	1.2×10^{-4}
75	8.0×10^{-6}
100	2.31×10^{-8}

As expected, Table 1 shows that the hydraulic conductivity has been reduced with the increase of VCI. This is because the free void space of the ballast is occupied by the fouling material.

2.2 Numerical Analysis using SEEP-W

A 2-D seepage analysis was conducted using a finite element software called SEEP-W (GeoStudio, 2007), to determine the drainage capacity with respect to various fouling conditions. Hydraulic conductivity values corresponding to different VCI obtained from experimental results were used as input parameters in the analysis. The vertical cross section of a typical Australian track, as shown in Figure 4, was used in this analysis, however, due to symmetry, only one half of the track has been considered.

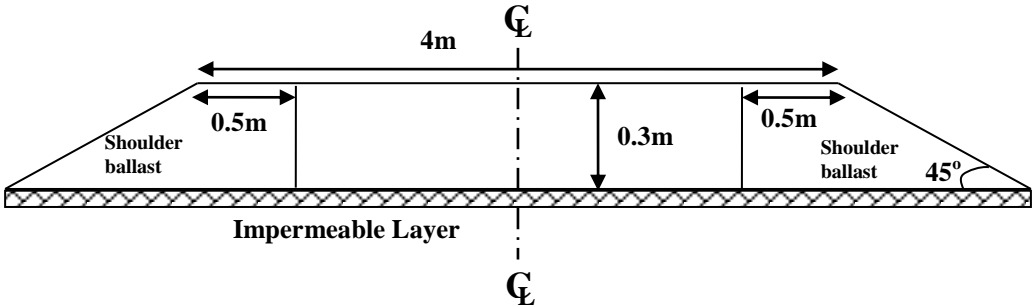


Figure 4: Vertical cross section of the typical ballast layer used in seepage analysis

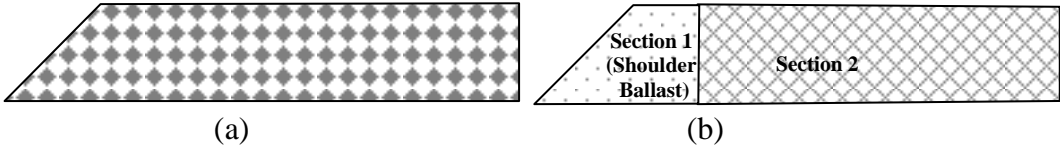


Figure 5: Fouled ballast patterns (a) Case 1, (b) Case 2

The values of hydraulic conductivity shown in Table 1 were used as input parameters in this analysis. In order to simulate two possible scenarios for track fouling, the following models for ballast fouled with clay were simulated.

Case 1: hydraulic conductivity values corresponding to different VCI values were used for the whole track (Figure 5a).

Case 2: Shoulder ballast was considered as separating the track into two sections (Figure 5b).

Table 2: Drainage capacity criteria (Tennakoon et al. 2012)

Drainage classification	Range
Free Drainage	$Q/Q_c > 100$
Good drainage	$10 < Q/Q_c < 100$
Acceptable drainage	$1 < Q/Q_c < 10$
Poor Drainage	$0.1 < Q/Q_c < 1$
very Poor	$0.001 < Q/Q_c < 0.1$
Impervious	$Q/Q_c < 0.001$

The drainage conditions of the track are classified as per criteria given by Tennakoon et al. (2012) and are given in Table 2. They used a maximum rainfall intensity of 150 mm/h and a corresponding flow rate named as critical flow rate (Q_c) of 0.0002 m³/s over the unit length of the track. From the seepage analysis, the maximum drainage capacity (Q) of the ballast can be determined for various levels of fouling for the above two models. When the drainage capacity of the track is equal to or lower than that required for a given rate of rainfall, then the fouled track drainage is classified as ‘poor drainage’. In this study a ratio between the computed track drainage capacity and the critical flow (Q/Q_c) was used as a dimensionless index to classify the drainage condition. Tables 3 and 4 present the results obtained from the analysis of cases 1 and 2 respectively.

Table 3: FE predictions for Case 1

VCI (%)	Q/Q_c	Drainage classification
0	110	Free Drainage
25	7.5	Acceptable Drainage
50	0.045	Very Poor Drainage
100	8.67×10^{-6}	Impervious

It is clear from Table 3 that when the whole track is fouled by more than 50% VCI, the drainage condition of the track is inadequate. A further investigation that considers the shoulder ballast (Table 4) implies that it can tolerate up to 25% VCI of fouling when the other section of the track is relatively clean (i.e. less than 25% VCI). However, if the shoulder ballast is fouled by more than 50% VCI, no matter how clean the other section of the track is, it creates a barrier to effective track drainage in every instance. Therefore, this analysis shows that keeping the shoulder ballast relatively clean is very important.

Table 4: FE predictions for Case 2

VCI (%)		Q/Q_c	Drainage classification
Section 1-Shoulder ballast (Figure 5b)	Section 2 (Figure 5b)		
0	25	42	Good Drainage
0	50	0.165	Poor Drainage
0	100	0.0000318	Impervious
25	25	7.5	Acceptable Drainage
25	50	0.161	Poor Drainage
50	0	0.11	Poor Drainage
100	0	0.0000175	Impervious

3 INFLUENCE OF TRAIN SPEED

The demand for high speed trains is increasing worldwide but any increase in speed exerts higher stresses on the ballast bed, and therefore the ballasted bed must be strong enough to withstand these additional stresses.

3.1 Large Scale Triaxial Tests

In order to understand the influence of train speed on ballast, a series of large scale triaxial tests (Figure 3) were carried out at the University of Wollongong. The testing was carried out at a 60 kPa confining pressure for frequencies of 10, 20, 30, and 40 Hz. The axial and volumetric deformations were recorded at different number of cycles during the test.

Figure 6 presents the variation of axial strain (ϵ_a) with the number of cycles (N). It is clear that the axial strains increase with increase of number of cycles and finally approach to a stable value. As the frequency increases the axial strain also increases. At an initial number of cycles ($N < 2500$) the axial strains appear to be increasing rapidly. It can be argued that this sudden increase in axial strains is due to particle re-arrangement and corner breakage. An increase in the frequency moves the stabilisation zone towards the left, which implies that at high frequency the ballast should experience more cyclic loading in order to stabilise.

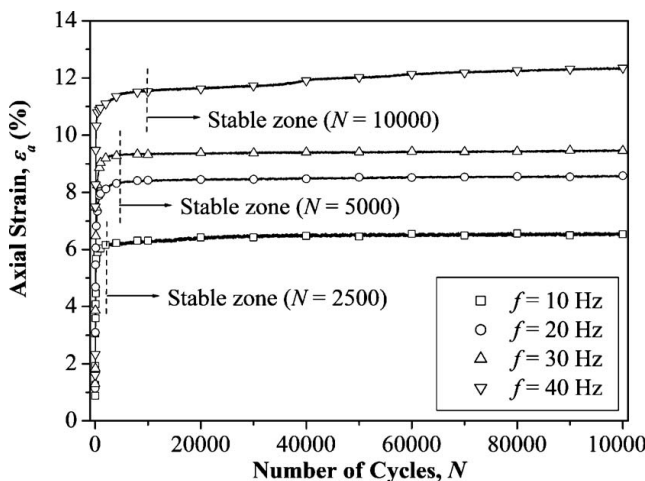


Figure 6: Variation of ϵ_a with N (data sourced from Indraratna et al. 2010)

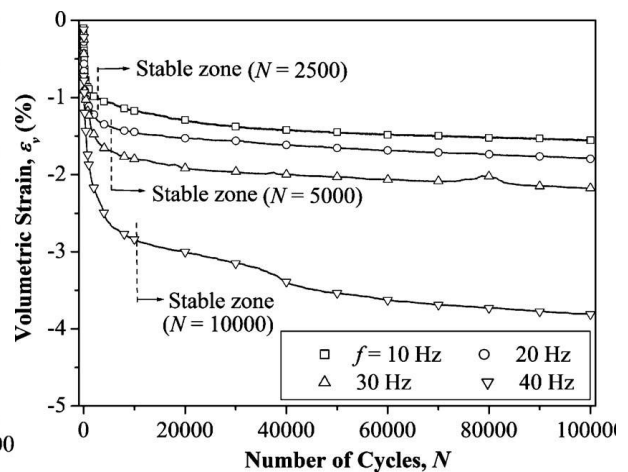


Figure 7: Variation of ϵ_v with N (data sourced from Indraratna et al. 2010)

Figure 7 illustrates the variation of volumetric strains (ϵ_v) with the number of cycles at different frequencies. At a low frequency ($f < 30$ Hz) the volumetric strains gradually increase to stable values at around 5000 cycles, whereas at high frequency ($f = 40$ Hz) the volumetric strains continually increase.

3.2 Numerical Analysis using DEM

A numerical simulation based on discrete element modeling (DEM), where the coarse angular grains are best represented as distinct particles, is presented in this paper. The dynamic analysis of Cundall and Strack (1979) in modeling circular or spherical particles is considered as the pioneering work in DEM. A new approach was followed by modeling the angularity of the ballast in the the particle flow code (PFC^{2D}). Sub-routines were developed (using the FISH Language) in PFC^{2D} after gathering the ID, radius, and coordinates of the centre of each circular particle that represent the irregular ballast particles and filler particles. These sub-

routines were used in the main program to generate irregular ballast particles (the particle sizes are between 19 mm and 53 mm). A typical sample considered for the cyclic biaxial tests is shown in Figure 8 (Indraratna et al. 2010).

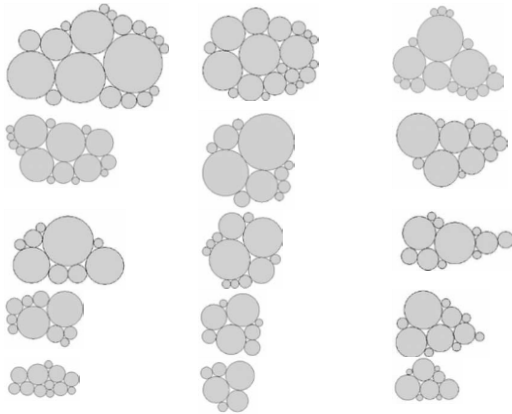


Figure 8: Particle sizes and shapes considered in the DEM (sourced from Indraratna et al. 2010)

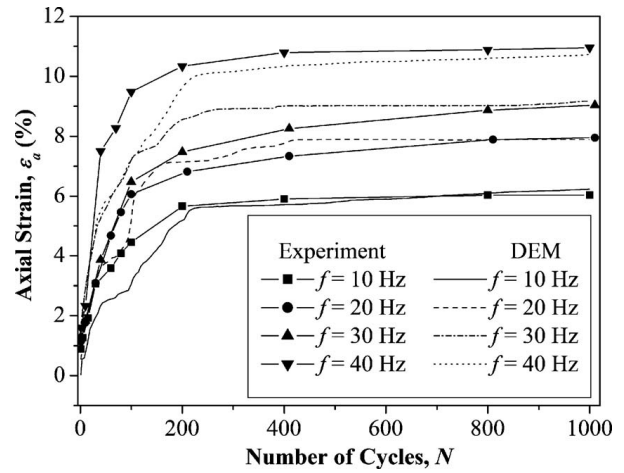


Figure 9: Comparison of ϵ_a observed in the experiment and in the DEM (data sourced from Indraratna et al. 2010)

In the analysis, 300 mm \times 600 mm biaxial cell was considered, and a linear contact model was used for the numerical simulation program. The angular aggregates are expected to behave in a manner that allows the particles to mainly slide together, while particle rotation was omitted. In this test, a moderate friction coefficient of 0.5 was used. The assembly was then subjected to 60 kPa of confining pressure. The sub-routine developed for stress controlled cyclic biaxial tests at a particular frequency was applied in the model. The DEM simulation was carried out up to 1000 cycles. Figure 9 shows the results of the DEM simulation and the experiment; and it is apparent that the DEM simulation is very close to the laboratory experiments carried out at various frequencies. It was clear from the numerical simulations that the frequency (train speed) of cyclic loading has a significant influence on the deformation of the ballast layer.

4 BEARING CAPACITY OF RAIL TRACK

In this section the limit equilibrium approach for determining the bearing capacity of rail track is presented.

4.1 Evaluation of Basic Friction Angle (ϕ_f) for Ballast

Indraratna and Salim (2002) proposed the following relationship to evaluate the basic friction angle (ϕ_f) of the ballast.

$$\frac{q}{p'} = \frac{\left(1 - \frac{d\epsilon_v}{d\epsilon_1}\right) \tan^2\left(45^\circ + \frac{\phi_{fb}}{2}\right) - 1}{\frac{2}{3} + \frac{1}{3}\left(1 - \frac{d\epsilon_v}{d\epsilon_1}\right) \tan^2\left(45^\circ + \frac{\phi_{fb}}{2}\right)} \quad (2)$$

where q/p' is the stress ratio, $(1-d\varepsilon_v/d\varepsilon_1)$ is the dilatancy, and ϕ_{fb} is apparent friction angle that includes a contribution from particle breakage but excludes the effect of dilatancy.

Using the triaxial data of stress ratio $(q/p')_f$ and dilatancy at failure $(1-d\varepsilon_v/d\varepsilon_1)_f$ in equation 2, the value of ϕ_{fb} were determined. The calculated ϕ_{fb} values were plotted against the initial confining pressure shown in Figure 10. It is evident that ϕ_{fb} increases at a diminishing rate with increasing confining pressure. The value of ϕ_f of the latite aggregates based on the triaxial testing is found to be approximately 44° ((Indraratna and Salim 2002).

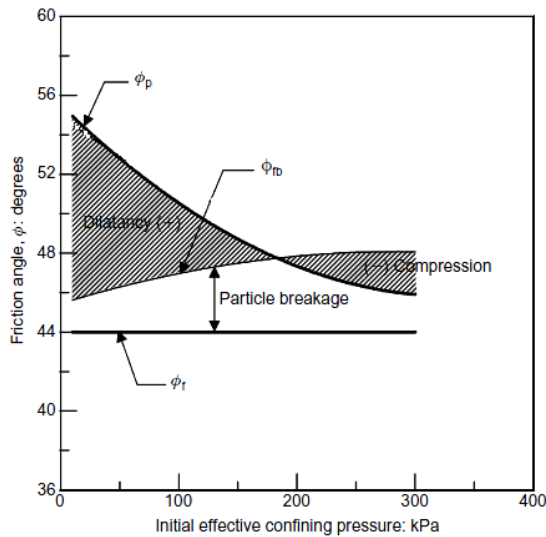


Figure 10: Effect of particle breakage, dilatancy and confining pressure on the friction angle (Indraratna and Salim 2002)

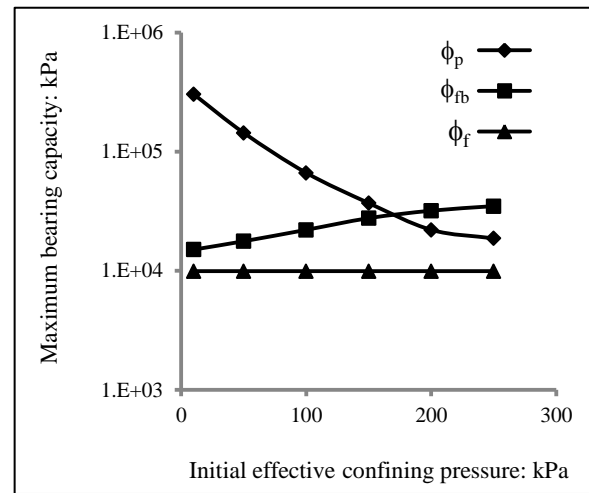


Figure 11: Effect of confining pressure on the maximum bearing capacity

4.2 Effect of Particle breakage on Peak Friction Angle

By rearranging the Mohr-Coulomb failure criterion and considering the peak principal stress ratio $(\sigma_1/\sigma_3)_p$, the peak friction angle could be conveniently calculated from the following relationship:

$$\left(\frac{\sigma'_1}{\sigma'_3}\right)_p = \frac{1 + \sin \phi_p}{1 - \sin \phi_p} \quad (3)$$

Figure 10 illustrates the values of various angles of friction with increasing effective confining pressure. The peak friction angle decreases with an increasing confining pressure. At a lower confining pressure the difference between ϕ_p and ϕ_{fb} becomes considerable because of the higher dilatancy, but at elevated confining pressures the difference between ϕ_{fb} and ϕ_f increases because of the higher rate of particle degradation. The peak friction angle ϕ_p , can therefore be considered as the summation of the basic friction angle ϕ_f , and the effects of dilatancy and particle breakage.

4.3 Bearing Capacity of Ballast

The maximum bearing capacity of the ballast V_{\max} , is obtained as (Le Pen and Powrie 2010):

$$V_{\max} = N_{\gamma} S_{\gamma} (0.5\gamma - \Delta u) BL \quad (4)$$

$$N_q = K_p e^{\pi \tan \phi} \quad (5)$$

$$K_p = \left(\frac{1 + \sin \phi}{1 - \sin \phi} \right) \quad (6)$$

$$N_{\gamma} = (N_q - 1) \tan(1.4\phi) \quad (7)$$

$$S_{\gamma} = 1 + 0.1K_p (B/L) \quad (8)$$

where γ is the bulk unit weight of ballast, Δu is the pore water pressure increment, B is the length of the sleeper, L is the width of the sleeper, ϕ is the angle of effective shearing resistance of the ballast, and N_q , N_{γ} and S_{γ} are the bearing capacity factors.

By using the various friction angles from Figure 11, together with $B = 2.5$ m, $L = 0.285$ m, $\gamma = 16$ kN/m³, $u = 0$, the maximum bearing capacity q_{\max} , can be calculated as shown in Figure 4. As the confining pressure increases the various bearing capacities of ballast show the same trends as the friction angles do in Figure 11.

5 THE BEHAVIOUR OF THE SUB-BALLAST (FILTER) UNDER CYCLIC TRAIN LOADING

In rail track environments the loading system is cyclic, unlike the static seepage force that usually occurs in embankment dams. The time dependent changes of the filtration properties require further research to improve the design guidelines. A standard testing procedure was established to monitor the performance of a granular filter which was previously identified as satisfactory based on existing criteria.

5.1 Experimental Methodology

To simulate dynamic train loading conditions applied onto a granular filter medium, a cyclic loading filtration apparatus was designed (Figure 12). The test apparatus consists of a chromium plated cylinder with an internal diameter of 240 mm, a wall thickness of 5 mm, and a height of 300 mm. The laboratory investigation was organised in 2 phases (Figure 13). In the first half of phase 1, non-slurry pseudo-static filtration tests were conducted to investigate the internal stability of the chosen filters (Kenney and Lau 1985). Pseudo-static tests are cyclic tests run at a frequency of 5 Hz, and they served as a control for the corresponding slurry filtration tests. Effluent turbidity readings were used to indicate internal stability. All filter types, including those that exhibited washout and poor drainage capacity, were subjected to slurry filtration tests during the second half of Phase 1. All these tests were terminated after 100,000 cycles.

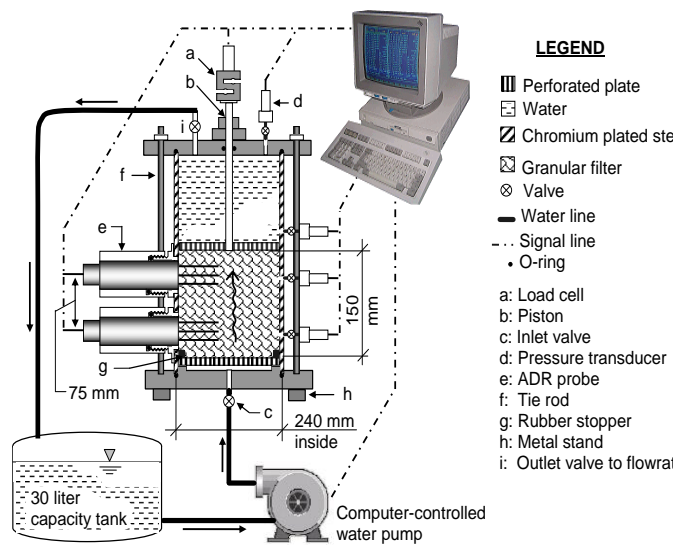


Figure 12: Cyclic loading permeameter (Trani and Indraratna 2010b)

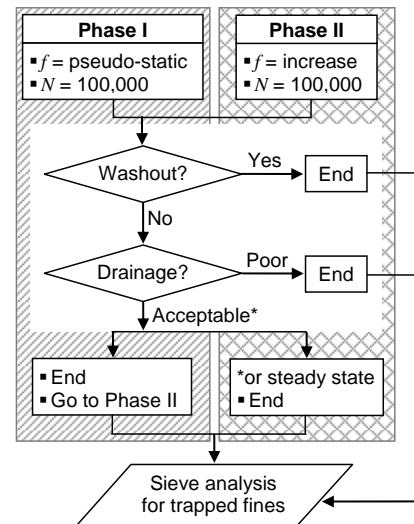


Figure 13: Experimental program

To simulate the filtration action in the event of clay pumping occurring in rail track environments, clay or silt slurry is pumped from the bottom of the setup while a cyclic load is applied from the top. A detailed soil specific calibration procedure is discussed by Trani and Indraratna (2010c). Through these probes, real time changes in the porosity of the filter are measured. Crushed basaltic rock road base material which is naturally well graded and has a uniformity coefficient (C_u) of 17 is used as granular filter sub-ballast. The angular road base material is carefully sieved into a range of particle sizes, washed, oven dried, and remixed into a predetermined particle size distribution (PSD). The base soil is a low plasticity and highly dispersive and erodible silty clay. To simulate a heavy haul train, a uniform cyclic stress in the form of a simple harmonic function is applied in an increasing frequency of 5, 10, 15, 20, and 25 Hz. Using a two dimensional stress distribution for a plane strain scenario, the train load is replicated in the modified permeameter using the dynamic actuator with a set of cyclic stresses applied to a minimum of 100,000 cycles. The specimen was subjected to a uniform minimum stress of 30 kPa and maximum stress of 70 kPa.

5.2 Test Results and Analysis

As shown in Figure 14a, rapid compression for all types of sub-ballast occurred during the first 7,500 cycles, irrespective of its grading or the range of particle sizes of which it is composed. The introduction of base soil during the slurry tests did not alter the development of strain in the filter (Figure 14b). Moreover, each type attains a stable configuration at about 20,000 cycles. The compressive behaviour allowed the void spaces of the filter medium skeleton to close up and hence, reduce the porosity. The amount of fines coming from the degradation of filter grains over time, which has the potential to become part of the filter skeleton or fill the voids, is insignificant. The average mass percentage of fines less than or equal to 150 μm produced after the test is less than 5%. This is best explained by the existence of optimum internal contact stress distribution and increased inter-particle contact areas.

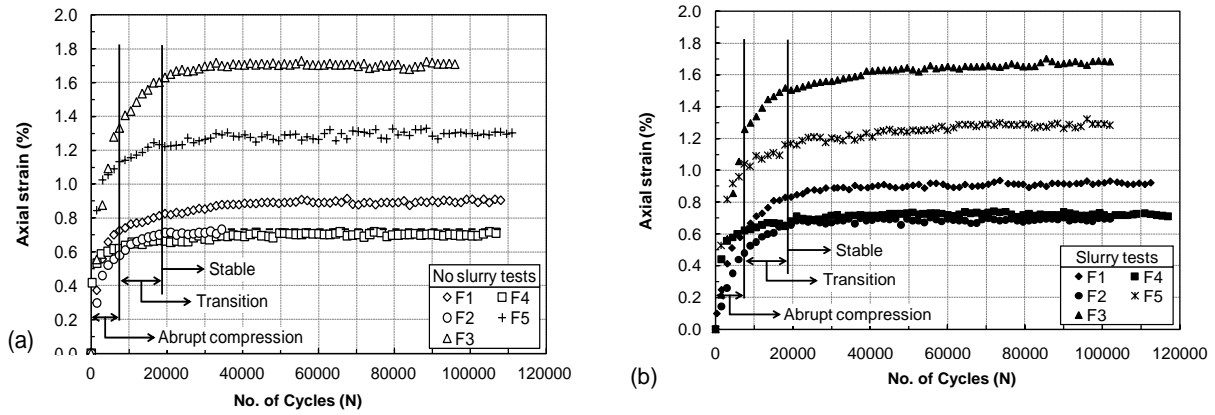


Figure 14: Accumulation of strain under cyclic loading for all filter types during (a) no slurry test, and (b) slurry tests (Trani and Indraratna 2010b)

6 FROM THEORY TO PRACTICE: FIELD STUDY AT BULLI

In order to assess the benefits of using geosynthetics in fresh and recycled ballast, a field trial was undertaken on a section of instrumented track at Bulli, NSW (Indraratna et al. 2010). The design specifications for the track were provided by the University of Wollongong and the field trial was sponsored by RailCorp, Sydney.

6.1 Track Construction

The field trial was carried out on a section of instrumented track located between two turnouts at Bulli, part of RailCorp’s South Coast Track. The total length of the instrumented track section was 60 m, which was divided into four 15m sections. The layers of ballast and sub-ballast were 300 mm and 150 mm thick, respectively.

6.2 Material Specifications

The particle gradation of fresh ballast was in accordance with the Technical Specification TS 3402 (RailCorp, Sydney). Recycled ballast was collected from spoil stockpiles of a recycled plant commissioned by RailCorp at Chullora yard near Sydney. The particle size distributions of fresh ballast, recycled ballast, and sub-ballast (capping) materials are given in Table 5.

Table 5: Grain size characteristics of ballast and sub-ballast (data sourced from Indraratna et al. 2010).

Material	d_{max} mm	d_{min} mm	d_{50} mm	C_u	C_c
Fresh Ballast	75.0	19.0	35.0	1.5	1.0
Recycled Ballast	75.0	9.5	38.0	1.8	1.0
Sub-ballast (capping)	19.0	0.05	0.26	5.0	1.2

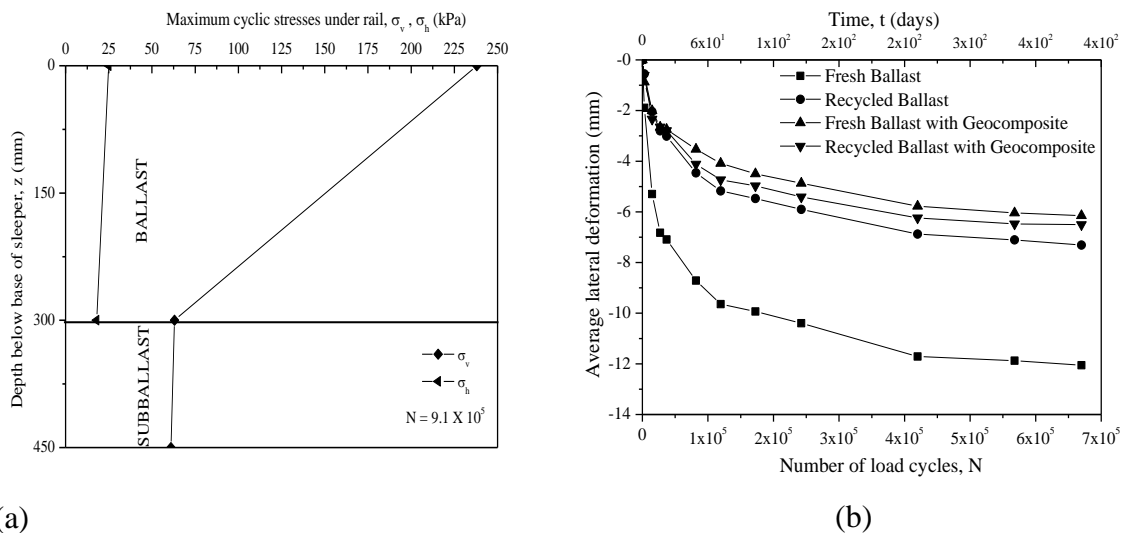
The layers of geocomposite consisted of bi-axial geogrids placed over layers of non-woven polypropylene geotextile. The technical specifications of the geosynthetic material used at this site have already been discussed by Indraratna et al. (2011b).

6.3 Track Instrumentation

The performance of the experimental section was monitored using a series of sophisticated instruments. The vertical and horizontal stresses developed in the ballast were measured by rapid response hydraulic earth pressure cells with thick, grooved, active faces based on semiconductor type transducers. Vertical and lateral deformations were measured by settlement pegs and electronic displacement transducers, respectively. These transducers were placed inside two, 2.5 m long stainless steel tubes that can slide over each other, with 100 mm × 100 mm end caps as anchors. The settlement pegs consisted of 100 mm × 100 mm × 6 mm stainless steel base plates attached to 10 mm diameter steel rods. The settlement pegs and displacement transducers were installed between the sleeper and ballast, and between the ballast and sub-ballast, respectively.

6.4 Traffic induced peak stresses and deformations in ballast

Figure 15a shows the maximum vertical cyclic stresses (σ_v) and maximum horizontal cyclic stresses (σ_h) recorded in Section 1, under the rail and the edge of the sleeper, from a passenger train travelling at 60 km/h (20.5 ton axle load). The large vertical stresses and relatively small lateral (confining) stresses caused large shear strains in the track.



(a) Figure 15: (a) Vertical and horizontal maximum cyclic stresses measured under the rail (σ_v, σ_h), (b) variation of average lateral deformation with number of load cycles (data sourced from Indraratna et al. 2010)

The average lateral deformations were determined from the mean of measurements between the sleeper and ballast, and between the ballast and sub-ballast. The average lateral deformations are plotted against the time scale (days) and number of load cycles (N) in Figure 15b. The recycled ballast showed less lateral deformations, because of its moderately graded particle size distribution compared to the very uniform fresh ballast. The ability of geosynthetics to reduce the rate of track deterioration is appealing to the railway industry.

7 FROM THEORY TO PRACTICE: FIELD STUDY AT SINGLETON

The sections of experimental track in this recent study were part of the Third (Relief) Track of the Minimbah Bank Stage 1 Line that extends from Bedford to Singleton, New South Wales.

7.1 Track Construction

Construction of the Third Track was started in July 2009 and the track was commissioned in May 2010. The Third Track was constructed to decrease the frequent traffic headway and harmonise this section of track with the remainder of the network. The Minimbah Bank Stage 1 Line is owned and operated by the Australian Rail Track Corporation (ARTC), and is mainly used to transport coal from mines in the Hunter Valley to the Port of Newcastle. The line also supports NSW Railcorp's light passenger trains servicing between Maitland and Scone. The locations of experimental sections on different parts of the Third Track are shown in Figure 16.

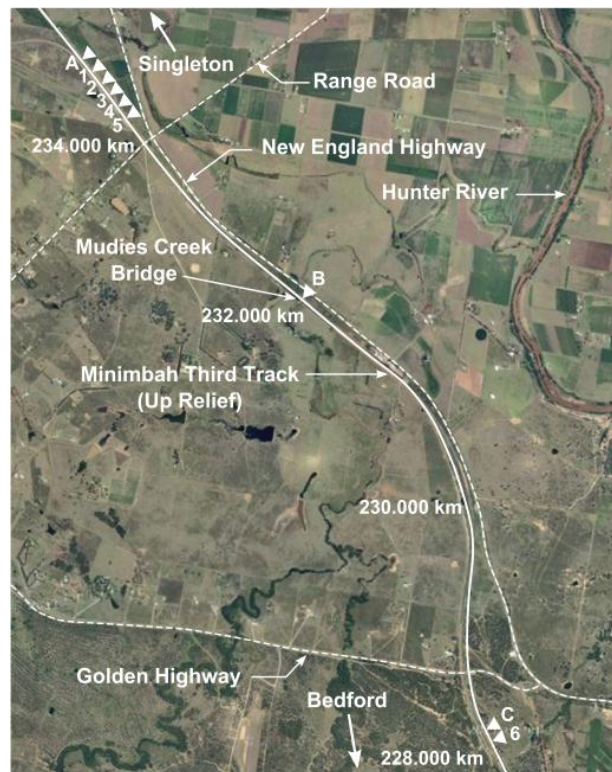


Figure 16: Locations of experimental sections on Minimbah Third Track.

7.2 Material Specifications

The substructure of the track consisted of a 300 mm thick layer of ballast (GP, angular latite basalt fragments, $d_{50} = 36$ mm,) underlain by a 150 mm thick layer of sub-ballast (GP-GM, compacted sandy gravel, $\text{CBR} \geq 50\%$, $d_{50} = 4$ mm). A structural layer of fill with a minimum of 500 mm thickness (GP-GM, compacted sandy gravel, $\text{CBR} \geq 30\%$, $d_{50} = 3$ mm) was placed below the sub-ballast. The gradation and classification of the ballast, sub-ballast, and structural fill materials are reported in Table 6.

Table 6: Gradation characteristics and USCS classification of test materials.

Material	Description	d ₅₀ (mm)	USCS classification	CBR (%)
Ballast	Compacted angular latite basalt	36	GP	-
Sub-ballast	Compacted sandy gravel	4	GP-GM	50
Structural fill	Compacted sandy gravel	3	GP-GM	30

Three commercially available geogrids and one geocomposite were installed in a single layer at the ballast-sub-ballast interface to investigate the key influential factors, i.e., the stiffness, aperture size, and filtration ability under ‘field’ conditions. A layer of shock mat was installed between the ballast and bridge deck to minimise any degradation of the ballast. The properties of the geosynthetics and shock mats used in this study are given in listed in Indraratna et al. (2012).

7.3 Track Instrumentation

Strain gauges were used to study deformations and mobilised forces along the layers of geogrid (Figure 17). Traffic induced vertical stresses were monitored by pressure cells. Transient deformations of the ballast were measured by five potentiometers (POTs) mounted on a custom built aluminum frame. Settlement pegs were installed between the sleeper and ballast and between the ballast and sub-ballast to measure vertical deformations of the ballast. The strain gauges were a post yield type suitable to measure tensile strains between 0.1 to 15%. Flexible aluminum sleeves were also used to protect the data cables of the strain gauges, as shown in Figure 17.

Pressure cells were installed at the sleeper-ballast and ballast-capping interfaces. During installation, the ballast was removed and the sub-ballast was levelled. The pressure cells were then placed in position and the ballast backfilled, as shown in Figure 18. The deformation frame was held in place by support bases installed in the sub-ballast and layers of structural fill. Figure 19 shows the deformation frame mounted in place to obtain any transient deformation of the ballast at Section A. Transient deformations were monitored at all the experimental sections, except for Section B.

Electrical analogue signals from the strain gauges, pressure cells, and potentiometers were obtained using a mobile data acquisition (DAQ) unit shown in Figure 20. The unit consisted of a National Instrument model 9188 module working in parallel with a mobile personal computer. The data acquisition module and associated wiring was housed in a custom made, aluminum case. The module provided electrical excitations and received signals from the instruments.

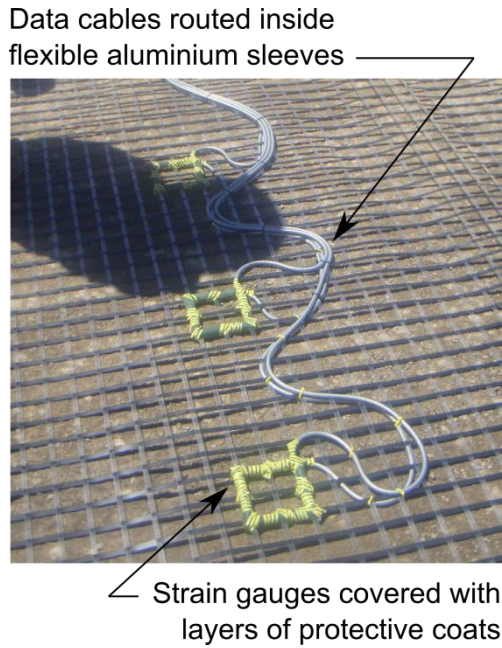


Figure 17: Strain gauges cables are covered in protective aluminum sleeves to avoid cuts from ballast particles.

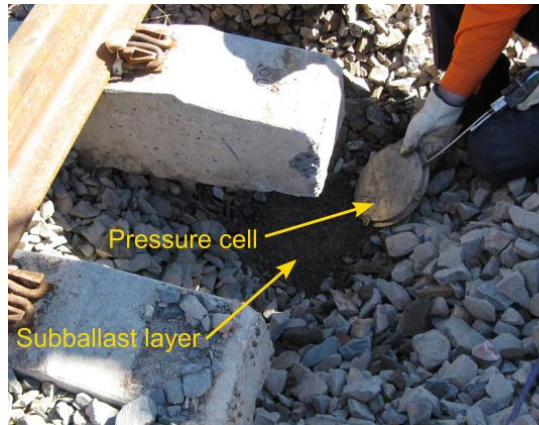


Figure 18: Installation of pressure cells involves removing and backfilling the ballast.

The input signals were amplified and filtered to reduce signal noises. These ‘conditioned’ signals were converted into a digital format and then later in real time in the mobile computer. The data acquisition module was configured and controlled by a computer program written in the National Instrument’s LabView environment. All the field data were obtained from the aforementioned instruments at a frequency of 2,000 Hz. A 12 V automotive battery provided a direct current power supply to the data acquisition module. Alternating power for the mobile computer was also provided by the same battery, but via an inverter.

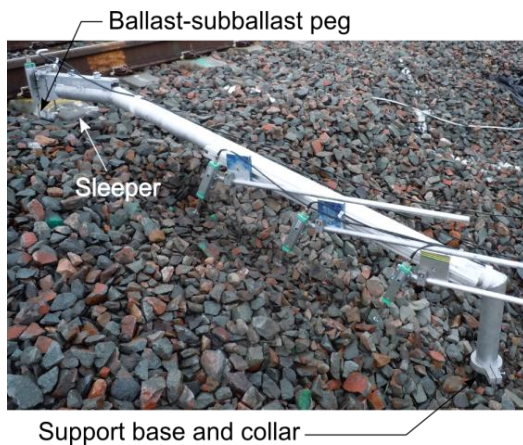


Figure 19: Displacement monitoring frame mounted on base.

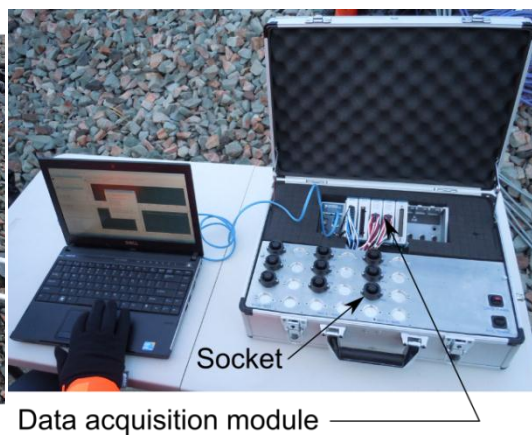


Figure 20: DAQ module connected to mobile personal computer.

7.4 Vertical Deformation of Ballast

The settlement (S_v) and vertical strain (ϵ_v) of the ballast after about 100,000 load cycles, or 40 days after the track was commissioned, and about 300,000 load cycles or 120 days, are reported in Table 7. These preliminary results indicate that the relationship between the settlement of ballast and the number of load cycles (N) is non-linear, regardless of how the track was reinforced. The rate at which settlements increased, decreased as the number of load cycles increased.

When the results for sections on similar subgrades were compared to each other, vertical deformations of the reinforced sections were 10-32% smaller than those without reinforcement. This pattern is similar to that observed in the laboratory (Shin et al. 2002 and Brown et al. 2007), and is mainly attributed to the interlocking between the ballast particles and grids, as discussed earlier. When the results for sections with similar geogrids are compared, it is apparent that the ability of geogrid reinforcement to reduce ballast deformation is generally higher for softer subgrades (low track substructure stiffness). Such an observation is in agreement with the results of the full scale laboratory tests presented by Ashmawy and Bourdeau (1995).

Moreover, of the four types of synthetics used, the geogrid at Section 4 performed most effectively. Although the stiffness of geogrid at this Section is equal to or lower than the others, its aperture size (40 mm) enabled better interlocking between the ballast particles and grids. This finding also agrees with the criteria for optimum size apertures for geogrids proposed by Brown et al. (2007) and Indraratna et al. (2011a). When Sections A, B, and C are compared, the results indicate that the vertical settlements are larger when the subgrade becomes weaker (low track stiffness), i.e., vertical settlement was smaller at the section on the concrete bridge deck (B) and larger than the section on the alluvial deposit (A).

Table 7: Vertical settlement and strain of the ballast layer.

(i) N = 100,000 load cycles									
Section	1	2	3	4	5	6	A	B	C
S_v mm	15.0	19.5	17.0	10.8	14.0	13.1	20.5	5.2	14.3
ϵ_v (%)	5.0	6.5	5.7	3.6	4.7	4.4	6.8	1.7	4.8
(ii) N = 300,000 load cycles									
Section	1	2	3	4	5	6	A	B	C
S_v mm	19.1	23.0	21.0	4.9	17.0	17.5	24.1	8.0	18.5
ϵ_v (%)	6.4	7.7	7.0	5.0	5.7	5.8	8.0	2.7	6.2

7.5 Transient Deformations of Ballast Layers

Transient deformations of the ballast layer were measured by the deformation frame. It was observed that the passage of trains with an axial load of 30 tonnes travelling at 40 km/h resulted in a vertical deformation (S_{tv}) between 1.5 to 3.0 mm, resulting in average vertical strain (ϵ_{tv}) of between 0.5 and 1.0%. The transient horizontal deformations of ballast (S_{th}) measured on the shoulder (up rail side) were all expansive and between -0.5 to -0.3 mm. This resulted in an average horizontal strain (ϵ_{th}) of -0.05 to -0.02%. The horizontal strains were

larger near the crest and smaller near the toe of the ballast. The average transient strains of track sections with reinforcement were about 15% smaller than those without reinforcement.

7.6 Traffic induced Vertical Stresses in Track

The vertical stresses (σ_v) due to the passage of trains with an axle load of 30 tonnes travelling at about 40 km/h were about 280 kPa at Section B (mat-deck interface) and between 30 to 40 kPa at Sections 1, 6, A, and C (ballast-sub-ballast interface). Vertical stresses at the sleeper-ballast interface of the latter sections were between 170 to 190 kPa, which indicate that the traffic-induced stresses were considerably larger in the track with a stiffer subgrade. The larger stresses also caused much more breakage of individual particles of ballast, as was anticipated. The ballast breakage index (BBI) after 750,000 load cycles for Sections B was 17%, while Sections A and C were 9.8% and 13.1%, respectively. This finding appears to contradict the general perception that ballast subjected to higher stresses (Section B) would undergo larger settlements and vertical strains due to larger degrees of particle breakage (Lackenby et al. 2007). This is because the ballast at Section B was contained within the barriers of the Mudies Creek bridge which meant that the ballast could not spread laterally. At Sections A and C however, the ballast was allowed to expand more freely in a horizontal direction, and larger vertical settlement was thus observed. This observation also confirms that the ability of ballast to expand horizontally also influences the magnitude of track settlement as well as the degree of ballast breakage.

7.7 Strains in Geosynthetics

Accumulated longitudinal (ϵ_l) and transverse (ϵ_t) strains after 100,000 and 300,000 load cycles, as measured by the bottom strain gauges installed below the edges of sleepers, are given in Table 8. Here, most of permanent strains in the geogrids in both directions developed when the track was being constructed, particularly when the ballast was being placed. In general, the strains did not change very much with the number of load cycles. As shown in Table 8, the transverse strains were generally larger than the longitudinal strains, probably due to confinement or a higher level of longitudinal restraint relative to the transverse direction. The values of ϵ_l and ϵ_t also appear to be mainly influenced by deformation of the subgrade. As also shown in the table, the transverse strains developed in the geocomposite (Section 5) were relatively large, although being stiffer they could have been expected to result in smaller strains because the embankment was constructed from alluvial silty clay and siltstone cuttings, and at this location underwent large lateral deformation shortly after the track was commissioned, which resulted in excessive transverse strains in the geocomposite.

Table 8: Typical values of accumulated longitudinal and transverse strains in geogrids.

(i) N = 100,000 load cycles						
Section	1	2	3	4	5	6
ϵ_l (%)	0.8	0.7	0.9	0.6	0.4	0.6
ϵ_t (%)	0.9	1.6	0.8	0.8	1.4	0.8
(ii) N = 300,000 load cycles						
Section	1	2	3	4	5	6
ϵ_l (%)	0.8	0.7	1.0	0.7	0.4	0.7
ϵ_t (%)	1.0	1.6	1.0	0.9	1.9	0.8

Induced transient strains in both the longitudinal ($\Delta\varepsilon_{lt}$) and transverse ($\Delta\varepsilon_{tt}$) directions due to the passage of trains with an axial load of 30 tonnes travelling at 40 km/h were between 0.14-0.17%. Unlike the accumulated strains, the values of $\Delta\varepsilon_{lt}$ and $\Delta\varepsilon_{tt}$ were smaller in grids with higher values of stiffness, but the transient strains in the geogrids were very consistent, and therefore were independent of the number of load cycles.

CONCLUSIONS

The performance of ballasted rail tracks with geosynthetic reinforcement and shock mats has been discussed through laboratory tests, theoretical modelling, field trials, and numerical simulations. The results highlight that particle breakage, confining pressure, frequency of cyclic loading, and soft formation in addition to train loading patterns (cyclic and impact) have a significant influence on the engineering behaviour of ballasted rail track.

The laboratory studies show that permanent deformation and degradation increased with the frequency and number of cycles. The DEM predictions were very close to the laboratory experiments carried out at various frequencies. The detrimental effects of fouling on the drainage characteristics were assessed using the VCI. It was shown that the VCI could accurately capture the fouling of ballast because it could incorporate the effects of void ratios, specific gravities, and gradations of both fouling material and ballast. Initially, even a small increase in the VCI leads to a significant decrease in the hydraulic conductivity of the fouled ballast.

The laboratory investigations on the sub-ballast filter shows that well graded sub-ballast is too porous to effectively capture the fines within its voids. It is recommended that uniformly graded sub-ballast with not more than 30% fine sand (particle range of 0.15 mm - 0.425 mm) has an enhanced filtering capacity. Due to the lack of mechanical resistance against axial deformation, the application of cyclic stress to uniformly graded sub-ballast results in a reduction in porosity that renders the filter more effective in trapping migrating fines.

The 'field' performance of ballasted rail tracks with geosynthetic reinforcement has been discussed in this paper. The performance of instrumented ballasted tracks at Bulli and Singleton was evaluated where different types of ballast and geosynthetic reinforcements were used. The results of the Bulli field study indicated that the use of geocomposites as reinforcing elements for tracks using recycled ballast proved to be a feasible and effective alternative. According to the results of the Singleton study, the effectiveness of geosynthetics appeared to increase, as the stiffness of the subgrade decreased. The strains accumulated in geogrids were influenced by deformation of the subgrade, while the induced transient strains were mainly affected by the stiffness of the geogrids. A better understanding of such a performance would allow for safer and more effective design and analysis of ballasted rail tracks with geosynthetic reinforcement.

ACKNOWLEDGEMENTS

The authors are grateful to the CRC for Rail Innovation for the funding of this research. The authors express their sincere thanks to Australian Research Council, RailCorp (Sydney), ARTC and Queensland Rail National for their continuous support. A number of current and past PhD students, namely Dr Joanne Lackenby, Dr Daniela Ionescu, Dr Wadud Salim, Dr Dominic Trani and Dr Pramod Kumar Thakur have participated to the contents of this paper and their contributions are greatly acknowledged. The Authors would like to thank Dr Pongpipat Anantanasakul (Lecturer, Mahidol University, Thailand). The authors would also

like to thank Mr. Alan Grant, Cameron Neilson and Ian Bridge of the University of Wollongong for their technical assistance throughout the period of this study. The on-site assistance provided by Mr. David Williams of ARTC is also appreciated. A significant portion of the contents have been reproduced with kind permission from the Journal of Geotechnical and Geoenvironmental Engineering ASCE, International Journal of Geomechanics, ASCE, ASTM Geotechnical Testing Journal, Geotechnique, and Canadian Geotechnical Journal.

REFERENCES

- Ashmawy, A. K. and Bourdeau, P. L., 1995. *Geosynthetic-reinforced soils under repeated loading: a review and comparative design study*. *Geosynthetics International*, 2(4): 643-678.
- Ashpiz, E. S., Diederich, R., and Koslowski, C., 2002. *The use of spunbonded geotextile in railway track renewal St Petersburg-Moscow*. Proceedings of the 7th International Conference on Geosynthetics, Nice, France, 1173-1176.
- Bathurst, R. J. and Raymond, G. P., 1987. *Geogrid reinforcement of ballasted track*. Transportation Research Board 1153, National Research Council, Washington D. C., 8-14.
- Brown, S. F., Kwan, J. and Thom, N. H. 2007. *Identifying the key parameters that influence geogrid reinforcement of railway ballast*. *Geotextiles and Geomembranes*, 25(6): 326-335.
- Cundall, P.A. and Strack, O.D.L., 1979. A discrete numerical model for granular assemblies. *Geotechnique*, 29, 47-65.
- GeoStudio, 2007. *SEEP/W for finite element seepage analysis, users manual*. Geo-Slope International Ltd, Calgary, Alberta, Canada.
- Indraratna, B. and Nimbalkar, S., 2012 *Stress-strain-degradation response of railway ballast stabilised with geosynthetics*. *Journal of Geotechnical and Geoenvironmental Engineering ASCE* (accepted, in press).
- Indraratna, B. and Salim, W., 2002. *Modelling of Particle Breakage of Coarse Aggregates Incorporating Strength and Dilatancy*. *Geotechnical Engineering*, 155(4): 243-252.
- Indraratna, B., and Salim, W., 2003. *Deformation and degradation mechanics of recycled ballast stabilised with geosynthetics* *Soils and Foundations*, 43(4): 35-46.
- Indraratna, B., Hussaini, S. K. and Vinod J. S., 2011a. *On the shear behaviour of ballast-geosynthetic interfaces*. *Geotechnical Testing Journal, ASTM* 35(2): 1-8.
- Indraratna, B., Khabbaz, H., Salim, W. and Christie, D., 2006. *Geotechnical properties of ballast and the role of geosynthetics in rail track stabilisation*. *Ground Improvement*, 10(3): 91-101.
- Indraratna, B., Lackenby, J., and Christie, D., 2005. *Effect of confining pressure on the degradation of ballast under cyclic loading*. *Geotechnique, UK*, 55(4): 325-328.
- Indraratna, B., Nimbalkar, S. and Rujikiatkamjorn, C., 2012. *Future of Australian rail tracks capturing higher speeds with heavier freight*, Sixteenth annual Symposium of Australian Geomechanics Society, Advances in Geotechnics of Roads and Railways, Sydney Chapter, 10 October 2012, Sydney, Australia: 1-24.
- Indraratna, B., Nimbalkar, S., Christie, D., Rujikiatkamjorn, C., and Vinod, J. S., 2010 *Field assessment of the performance of a ballasted rail track with and without geosynthetics*. *Journal of Geotechnical and Geoenvironmental Engineering, ASCE*, 136(7): 907-917.
- Indraratna, B., Salim, W., and Rujikiatkamjorn, C., 2011b *Advanced Rail Geotechnology – Ballasted Track*: CRC Press/Balkema.
- Indraratna, B., Shahin, M. A., and Salim, W., 2007. *Stabilising granular media and formation soil using geosynthetics with special reference to Railway engineering*. *Ground Improvement*, 11(1): 27-44.

- Indraratna, B., Tennakoon, N., Nimbalkar, S., and Rujikiatkamjorn, C., 2012 *Behaviour of Clay Fouled Ballast under Drained Triaxial Testing*. Geotechnique, 62(10) (in press).
- Indraratna, B., Thakur, P. K. and Vinod, J. S., 2010. *Experimental and Numerical Study of Railway Ballast Behavior under Cyclic Loading*. International Journal of Geomechanics, 10(4), 136-144.
- Jenkins, H. M., Stephenson, J. E., Clayton, G. A., Morland, J. W., and Lyon, D., 1974. *The effect of track and vehicle parameters on wheel/rail vertical dynamic forces*. Railway Engineering Journal, 3: 2-16.
- Kenney, T. C. and Lau, D., 1985. *Internal stability of granular filters*. Canadian Geotechnical Journal, 22(2): 215-225.
- Lackenby, J., 2006. *Triaxial behavior of ballast and the role of confining pressure under cyclic loading*, University of Wollongong, Australia, PhD Thesis
- Lackenby, J., Indraratna, B., McDowell, G., and Christie, D., 2007. *Effect of confining pressure on ballast degradation and deformation under cyclic triaxial loading*. Geotechnique, 57(6): 527-536.
- Le Pen, L. M. and Powrie, W., 2010. *Contribution of Base, Crib, and Shoulder Ballast to the Lateral Sliding Resistance of Railway Track: a Geotechnical Perspective*. Proceedings of IMechE, Vol. 225, Part F: Journal of Rail and Rapid Transit, Special Issue Paper, 113-128.
- Li, D. and Selig, E. T., 1998. *Method for Railroad Track Foundation Design: Development*. Journal of Geotechnical and Geoenvironmental Engineering ASCE, 124(4): 316-322.
- Marsal, R. J., 1973. *Mechanical properties of rock fill*. In: Hirschfield R. C. and Pools, S. J. (eds) Embankment Dam Engineering: Casagrande Volume, Wiley, New York, 109-200.
- Nimbalkar, S., Indraratna, B., Dash, S. K., and Christie, D., 2012. *Improved performance of railway ballast under impact loads using shock mats*. Journal of Geotechnical and Geoenvironmental Engineering ASCE, 138(3): 281-294.
- Profillidis V. A., 1995 *Railway Engineering*. Avebury Technical, Aldershot.
- Raymond, G. P., 2002. *Reinforced ballast behaviour subjected to repeated load*. Geotextiles and Geomembranes 20(1): 39-61.
- RCA Australia, 2008. *Geotechnical Investigation Report for Minimbah Bank Third Track*. RCA Australia, Newcastle, Australia.
- Rowe P. K. and Jones C. P., 2000. *Geosynthetics: innovative materials and rational design*. In: Proceedings, GEOENG 2000, Melbourne, Australia, 1124-1156.
- Selig, E. T., and Waters, J. M., 1994. *Track Geotechnology and Substructure Management*, Thomas Telford, London. Reprint 2007.
- Shin E. C., Kim D. H. and Das B. M., 2002. *Geogrid-reinforced railroad bed settlement due to cyclic load*. Geotechnical and Geological Engineering, 20(3): 261-271.
- Standards Australia., 1996. *Aggregates and rock for engineering purposes*, Part 7: Railway ballast AS 2758.7-1996. Sydney, NSW, Australia.
- Tennakoon, N., Indraratna, B., Rujikiatkamjorn, C., Nimbalkar, S., and Neville, T., 2012 *The role of ballast-fouling characteristics on the drainage capacity of a rail substructure*. Geotechnical Testing Journal, 35(4):1-12.
- Trani, L.D.O. and Indraratna, B., 2010a. *Assessment of subballast filtration under cyclic loading*. Journal of Geotechnical and Geoenvironmental Engineering ASCE, 136(11): 1519-1528.
- Trani, L.D.O. and Indraratna, B., 2010b. *Experimental investigations into subballast filtration behavior under cyclic conditions*. Australian Geomechanics Journal, 45(3): 123-133.
- Trani, L.D.O. and Indraratna, B., 2010c. *The use of impedance probe for estimation of porosity changes in saturated granular filters under cyclic loading: calibration and application*. Journal of Geotechnical and Geoenvironmental Engineering, ASCE, 136(10): 1469-1474.